Eur Biophys J (1997) 26: 253–259

ARTICLE

Miguel A. R. B. Castanho · Nuno C. Santos
Luís M. S. Loura

Separating the turbidity spectra of vesicles from the absorption spectra of membrane probes and other chromophores

Received: 22 November 1996 / Accepted: 13 March 1997

Abstract The recording of the absorption spectra of membrane probes and other chromophores is frequently difficult because of turbidity. While in highly scattering media such as tissues, the solution to the problem can be rather complex, in cell and vesicle suspensions it can be quite simple. In this work we aim to demonstrate that the "blurred" sum spectrum can be decomposed into the absorption and turbidity spectra using very well defined theoretical models rather than blind empirical procedures and intuition. Basically, the methodology consists in the fitting of a power law to an absorption – free segment of the total spectrum. The power parameter is related to the dimensions, refractive index and size polydispersity of the scattering particles. The proposed methodology was applied to a polyene sterol probe in lipid vesicles (both uni and multilamellar).

Key words Turbidity · Absorption spectrum · Membrane probe · Vesicle · Dehydroergosterol

Introduction

UV-Vis spectroscopy techniques, such as absorbance and fluorescence are often used to study membrane structure and fluidity, protein lipid interaction and a wide variety of other membrane related phenomena (for a collection of reviews on these subjects see, e.g., Loew 1988). Whether one is studying intrinsic chromophores, such as Trp or Tyr residues in proteins, or inserted probes, a need exists to quantify concentration and/or to obtain structural information such as, e.g., transition energies, solvatochromic shifts and exciton interaction. Whatever the reason may be, the use of absorption spectra is often critical. However, membrane systems are big and have relative refractive indexes that differ from unity. Thus, reliable absorption spectra are difficult to obtain owing to turbidity, even if lipid vesicles are used instead of cells. Technical solutions have been proposed to record absorption spectra in moderately turbid media. One of them consists of the integrating sphere: the sample is placed on the edge of a hollow sphere that is covered by MgO on the inside (or other material of high diffuse reflectance such as $BaSO_4$, for example). The MgO efficiently reflects the light, regardless of the wavelength. The incident beam impinges on the sample cell from the outside to the inside of the sphere. The light scattered in the forward direction is then reflected from the inner surface of the sphere and directed towards the detector. Unfortunately, poor signal to noise ratios are obtained with this system and prices are prohibitive for most users. Not surprisingly, this technique is not widely used. An alternative approach is available: By increasing the proximity of the sample cell to the detector[1] and increasing the size of the active area ("collecting" area) of the detector, it is possible to make a significant fraction of the scattered light reach the photomultiplier. The system works as if such a fraction of the scattered light had never been scattered. It should be remembered that large particles scatter light preferentially in the forward direction; thus, the fraction of scattered light collected is larger than the solid angle fraction of the collecting system suggests. However, the most common and widely used UV-Vis absorption spectrophotometers are not suited for short sample – detector distances and do not have detectors with big active areas. In addition, in the case of a strongly fluorescent solution the absorption signal is biased. Moreover, equipment available with these modifications is very expensive.

A simple and inexpensive alternative approach is to separate turbidity from the true absorption in the spectra ob-

M. A. R. B. Castanho (✉) · N. C. Santos · L. M. S. Loura
Centro de Química Física Molecular, Instituto Superior Técnico, Av. Rovisco Pais, P-1096 Lisboa Codex, Portugal
(Fax +351 1 3524372/3536985;
e-mail: pcmcastanho@alfa.ist.utl.pt)

M. A. R. B. Castanho · N. C. Santos
Faculdade de Ciências da Universidade de Lisboa, Departamento de Química e Bioquímica, Campo Grande, P-1700 Lisboa, Portugal

[1] The solid angle increases linearly with r^{-2} (r is the sample – detector distance)

tained from ordinary spectrophotometers. Separating turbidity from the true absorption in a "blurred" spectrum is usually based on common empirical procedures rather than on a theoretical scientific approach. Nevertheless, the problem can be easily handled by considering simple and basic light scattering concepts. In this work we aim to demonstrate that the "blurred" sum spectrum can be decomposed into the absorption and turbidity spectra according to very well defined theoretical models. In addition, the conditions necessary to make the procedure valid are clearly defined.

Theoretical background

Turbidity, τ, is defined as:

$$\tau = -\ln \frac{I}{I_0} \tag{1}$$

(I_0 is the incident beam intensity and I is the transmitted beam intensity). Therefore, the pseudo absorbance signal, A′, read in an absorption spectrophotometer is related to turbidity by:

$$\tau = 2.303 \cdot A' \tag{2}$$

τ can be regarded as an extinction coefficient that attenuates the beam passing through the sample cell. The formalism is similar to the one used to derive Lambert-Beer's law. Only the physical phenomena are different: in one case light is absorbed while in the other it is scattered. The incident beam is attenuated in the same way (e.g., van de Hulst 1981). Nevertheless, this does not mean that true and pseudo-absorption (scattering) are always additive. In fact, absorption is a single event (the same photon cannot be absorbed more than once) so the absorbed photons will never reach the detector[2]. In contrast, light scattering may happen in multiple events (the same photon may be scattered several times in the sample volume before escaping from the sample cell boundaries). A photon may therefore be scattered several times and reach the detector if the final scattering event occurs in the detector direction. If an absorbing sample is used, the scattered photons are more likely to be absorbed because they have increased light paths. Such a complex scenario cannot be accounted for by simple additivity of the absorption and turbidity-related phenomena (pseudo-absorption). More complex and demanding analysis has to be performed (e.g., Fantini et al. 1994; Wu et al. 1993; Bonner et al. 1987). However, unless the work has to be carried out in tissues or other strongly scattering media, conditions can be set so that multiple scattering does not occur. A simple way to guarantee the absence of multiple scattering is to check on the linearity between pseudo-absorption and concentration. In the linear relationship concentration interval, multiple scattering is not significant and the absorption spectrum can be obtained by subtraction ($A(\lambda) = T(\lambda) - A'(\lambda)$, where $T(\lambda)$ is the total spectrum).

It is necessary to address the problem of the computation of $A'(\lambda)$ according to the scattering particle size:

1 Rayleigh-Gans approach

The Rayleigh-Gans (RG) approach is valid for small particles with a relative refractive index ($m = n_P/n_S$; n_P is the refractive index of the scattering particle and n_S is the refractive index of the solvent) close to unity. Namely (e.g., van de Hulst 1981):

$$|m-1| \ll 1 \tag{3}$$

$$\frac{4\pi}{\lambda} a\,|m-1| \ll 1 \tag{4}$$

(a is a length of the magnitude of the size of the particle; it is sometimes referred to as the typical length of the particle: a is the radius in the case of a sphere or the length, in the case of a cylinder, for instance). With these assumptions, the following equations are valid (Yoshikawa et al. 1983):

$$\tau = \tau_R \frac{3}{8} \int_0^{\pi} P(\theta)\,(1+\cos^2\theta)\sin\theta\,d\theta \tag{5}$$

$$\tau_R = \frac{32}{27}\pi^3 \left(\frac{\partial n_p}{\partial C}\right)^2 \frac{w^2 N n_s^2}{\lambda^4} \tag{6}$$

N is the number concentration of particles in the sample, w is the scattering particle mass and $P(\theta)$ is the intraparticle scattering factor, which accounts for the interference of light scattered from different parts of the particles, according to the measurement angle. $P(\theta)$ depends on the size and shape of the particle. For smal sizes ($a \ll \lambda$), $P(\theta)$ approaches 1. In this case, $\tau = \tau_R$ where τ_R is the turbidity expected from Rayleigh scattering (i.e. the particles can be considered as point scatterers).

As $P(\theta)$ is a structure dependent factor, to proceed with our analysis, one has to consider several cases separately:

1.1 Unilamellar vesicles

The scattering model for unilamellar vesicles is the hollow sphere (Fig. 1 a) which takes the form (e.g., Schmitz 1990):

$$P(\theta) = \left[\frac{3}{x^3(1-\gamma^3)}\left[\sin x - \sin(\gamma x) - x\cos x + \gamma x \cos(\gamma x)\right]\right]^2 \tag{7}$$

$$\gamma = R_1/R_2 \tag{8}$$

$$x = q \cdot R_2 \tag{9}$$

$$q = (4\pi n_S/\lambda)\sin(\theta/2) \tag{10}$$

where R_1 and R_2 are the inner and outer radius of the hollow sphere (Fig. 1 a).

[2] Even if the chromophore decays radiatively and emits fluorescence involving some photons with the same energy as the exciting photon, the probability that such photons are emitted in the detector direction is very low

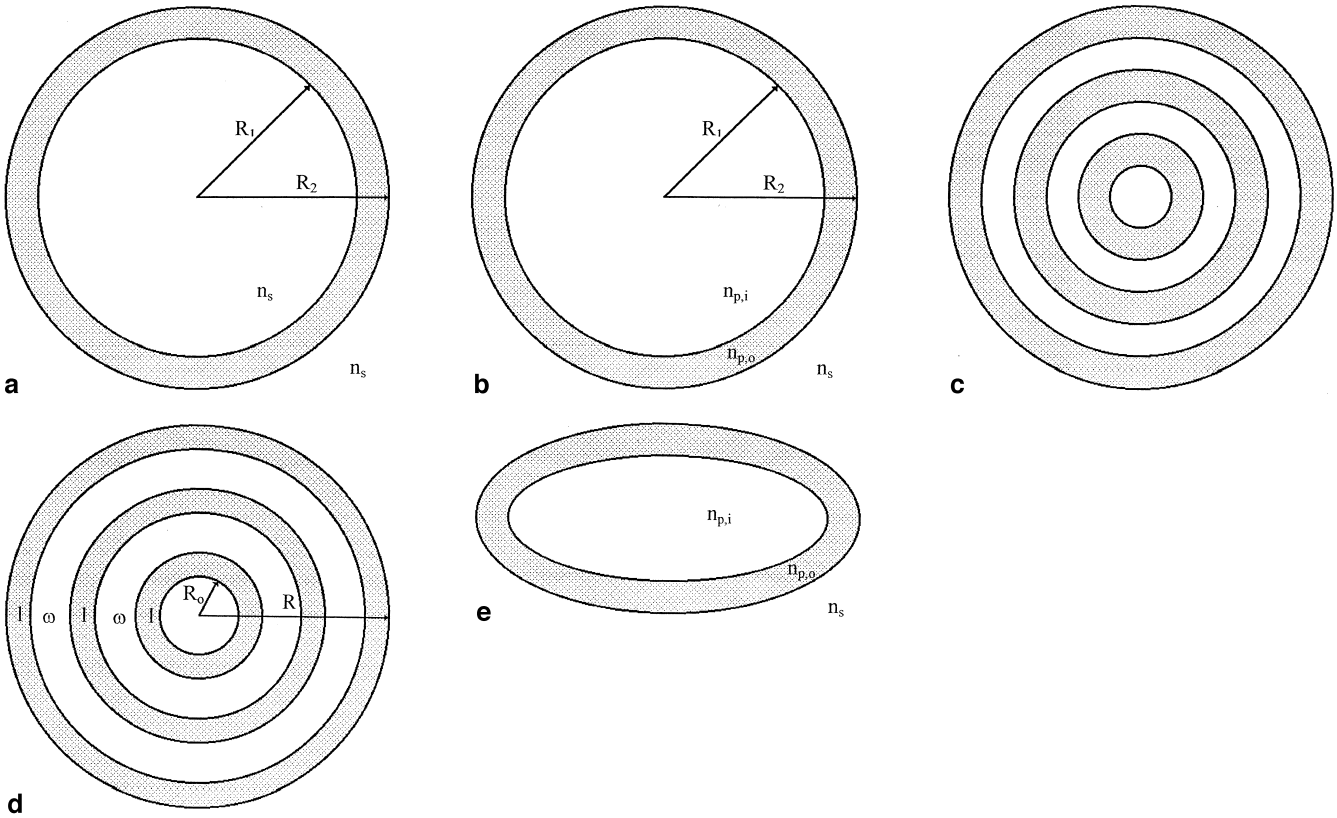

Fig. 1 Model geometries used to predict and explain the scattering properties of lipidic vesicles (**a**–**d**) and cells (**e**). **a** Hollow sphere model. A sphere of solvent having radius R_1 is surrounded by a spherical shell of the solute, having external radius R_2. **b** Coated sphere model. An inner homogeneous sphere of refractive index $n_{P,i}$ and radius R_1 is surrounded by a concentric shell of refractive index $n_{P,o}$ and outer radius R_2. The medium refractive index is n_s. **c** Multi-shelled sphere model. The thickness of each lipid and each water shell is assumed to be the same (Yoshikawa et al. 1983). For the sake of simplicity only three lipid shells were represented. However, it is worth stressing that MLV generally consist of five or more lipid shells (New 1990). **d** Chong and Colbow (1976) model for a multi-lamellar vesicle. A series of concentric lipid shells, each of thickness 1, encloses solvent layers of thickness ω and an inner solvent core. As in **c**, only three lamellae are represented, for the sake of simplicity. **e** Two-layered spheroidal particle (Wang et al. 1979). An inner homogeneous prolate spheroid particle is surrounded by a coat of constant thickness and different refractive index

If γ is close to unity then Eq. (7) can be simplified to:

$$P(\theta) = \left(\frac{\sin x}{x}\right)^2 \tag{11}$$

In the case where the vesicle interior is not filled with pure solvent, but with a solution or suspension of a different refractive index, another scattering model has to be considered: The coated sphere model (Fig. 1 b). In this case (e.g., Kerker 1969):

$$P(\theta) = \left[\frac{3 j_1(qR_2)}{qR_2} + \left(\frac{m_1 - m_2}{m_2 - 1}\right)\left(\frac{R_1}{R_2}\right)^3 \frac{3 j_1(qR_1)}{qR_1}\right]^2 \tag{12}$$

where $j_1(qR_n)$ is the first order spherical Bessel function and $m_1 = n_{P,i}/n_S$ and $m_2 = n_{P,o}/n_S$.

If the coated sphere model is to be used, the conditions described by Eqs. (3) and (4) should be valid for both inner core relative to the coat and coat relative to the solvent.

$P(\theta)$ can be computed in both cases provided that the dimensions of the vesicles are known. If a spectral study is one's only concern, the basic idea to retain is that the turbidity is approximately proportional to the inverse of the fourth power of the wavelength, provided that the refractive indexes are not strongly wavelength dependent.

1.2 Multi-lamellar vesicles

Turbidimetry studies on multilamellar vesicles were performed carefully by Yoshikawa et al. (1983), who considered the model of a multi-shelled sphere (Fig. 1 c). The results suggest, however, that the turbidity of a multi-shelled sphere suspension is approximately the same as that of homogenous spheres of average refractive index. That is to say that n_P is substituted by $\bar{n}$ in Eq. (6) and $P(\theta)$ is that of a homogeneous sphere:

$$P(\theta) = \left[\frac{3}{(qR)^3}\left[\sin(qR) - qR\cos(qR)\right]\right]^2 \tag{13}$$

(R is the radius of the sphere). As the RG approach is only valid if n_P/n_S is close to unity, one can use a simple average of the refractive indexes:

$$\bar{n} = f_P n_P + (1 - f_P) n_S \tag{14}$$

(f_P is the volume fraction of the scattering material on the particle).

Chong and Colbow (1976) have also considered the turbidity caused by multilamellar vesicles within the framework of the RG approach. The scattering model considered by these authors is more general than the one presented in Fig. 1 c. Chong's model considers y concentric lipid shells each of thickness t enclosing solvent of thickness ω between the shells and an inner core of solvent having radius R_0 (Fig. 1 d). In this case:

$$P(\theta)=\left\{\frac{4\pi}{q^3V}\sum_{j=1}^{y}[\sin q x'_j-\sin q(x'_j-t) + q(x'_j-t)\cos q(x'_j-t)-q x'_j\cos q x'_j]\right\}^2 \qquad (15)$$

where $x'_j=R_0+(j-t)\omega+jt$ and V is the total volume of lipid in the vesicle:

$$V=\frac{4\pi}{3}\sum_{j=1}^{y}[x'^3_j-(x'_j-t)^3] \qquad (16)$$

Whatever model is considered, τ is approximately proportional to λ^{-4}; this is also true for multilamellar vesicles, as long as the refractive indexes are not strongly wavelength dependent and Eqs. (3) and (4) are valid.

1.3 Cells

Cells are very unlikely to fulfil the requirements of the RG approach (Eqs. (3) and (4)) but, nevertheless, it is known that the RG approach can sometimes give fairly good results even if its assumptions are not obeyed (e.g., Kerker 1969; Wang et al. 1979). In any case the reader should be aware that the error in the RG approximation increases with the particle scattering size of the spheres and that deviations from the spherical geometry further increase the error (Barber and Wang 1978). The scattering model to be used is the coated sphere model (Fig. 1 b). Wang et al. (1979) extended the model to prolate spheroidal particles (Fig. 1 e) and studied the influence of size polydispersity on the angular profile of the light scattering intensity. Although Wang et al. have considered an incident beam of polarised light (at variance with the situation in standard spectrophotometers, which use unpolarised light [3]) a basic idea could be considered: The integrated intensity over the measurement angle might not differ much from other more precise approaches.

As before, the predicted turbidity is still approximately proportional to λ^{-4}. The RG approach predicts this kind of dependence whatever scattering model is considered from those of Fig. 1 a–e.

[3] Ideally, the light should be strictly unpolarised; in reality, monochromators impose a partial vertical polarisation

2 Mie approach

The Mie approach to light scattering does not require the restrictive assumptions involved in the RG approach (Eqs. [3] and [4]). The scattering of light by a homogenous particle can be treated in a general way by the formal solution of Maxwell's equations with the appropriate boundary conditions (van de Hulst 1981). Nevertheless, the calculations involved are complex and its application to geometries other than spheres is difficult. Yoshikawa et al. (1983) studied the application of Mie's theory to the multishelled sphere model (Fig. 1 c), including the special case of a hollow sphere (Fig. 1 b). A systematic study of a sphere with the same radius but with different lipid shell numbers (1 to 10) at a given lipid fraction was carried out. The scattering efficiency is determined mainly by the volume ratio of the two scattering media (lipid and water, in the case of vesicles). Using typical values for n_P (namely, the value for egg yolk lecithin at 20 °C and 436 nm; $n_P=1.497$), the scattering efficiency is insensitive to the inner core structure.

The numerical calculations involved in Mie's approach are too complex for the purpose of the present work (to separate the contributions of turbidity and "true" absorption in a spectrum). However, if:

$$1 \ll \frac{2\pi n_S R}{\lambda} \ll \frac{1}{\bar{m}-1} \qquad (17)$$

(R is the radius and $\bar{m}=\bar{n}/n_S$), the turbidity equals (e.g., Yoshikawa et al. 1983):

$$\tau=\frac{9}{2}\pi\left(\frac{\partial\bar{n}}{\partial C}\right)^2\frac{w^2N}{R^2\lambda^2} \qquad (18)$$

$\bar{n}$ can be obtained from the sum rule of polarisability:

$$\frac{\bar{n}^2-1}{\bar{n}^2+2}=f_P\frac{n_P^2-1}{n_P^2+2}+(1-f_P)\frac{n_S^2-1}{n_S^2+2} \qquad (19)$$

Besides being size dependent ($\tau\propto R^2$), the turbidity is now proportional to λ^{-2}, instead of λ^{-4} as in the RG approach.

Methodology

We have seen that pseudo-absorption is proportional to λ^{-k}, k being a size dependent value. If the RG conditions are fulfilled: k=4; if Eq. (17) is fulfilled: k=2. However, k is also dependent on the scattering particle size distributions and decreases with increasing particle size distribution standard deviation. k approaches 1 for an infinitely large standard deviation (provided that n_P is not dependent on λ) (Yang and Hogg 1979). The size distributions of unilamellar vesicles (sonicated or extruded) and cells are expected to be narrower than those for MLV (multilamellar vesicles). However, even in the former cases it may not be easy to compute τ because of the parameters in Eqs. (5),

(6) and (18). Therefore, we recommend an alternative procedure to subtract pseudo-absorption from the total spectrum (remembering to check for the absence of multiple scattering):

(1) Record the absorption spectrum including a λ range with lower energies, where true absorption does not occur (use the solvent alone for baseline correction).
(2) Using nonlinear regression methods, fit the equation $A' = B + K_0 \cdot \lambda^{-k}$ to the experimental data outside the true absorption region (K_0 and k are constants). B should be zero unless baseline errors occur[4].
(3) Extrapolate the equation obtained in (2) to the whole λ range[5].
(4) Subtract the extrapolated function from the experimental spectrum. The result is the true absorption spectrum.

If might seem that automatic baseline correction does the same job. Alternatively, if a dual beam spectrophotometer is being used, automatic blank subtraction can be carried out and the above procedure might seem avoidable and pointless. However, in practical terms, two kinds of situation are very common:

a) The samples are too turbid and a precise baseline cannot be determined. If the UV range is used this is a likely situation since A′ might increase with steep gradients (recall that $A' \propto \lambda^{-4}$ for small particles), leading to very imprecise baselines (subtracting two signals in these conditions creates random errors of large magnitude). Moreover, if a baseline is determined then it is obtained from a very attenuated signal, having low signal to noise ratios.
b) Chromophore bearing molecules (such as proteins and peptides, for instance) may induce refractive indexes changes, volume changes (such as swelling or shrinking of the vesicles, or even fusion) or shape alterations. In this case, the turbidity spectrum of the sample may differ significantly from that of the blank.

These two problems do not exist if the recommended procedure is followed: The baseline is established with non-scattering media (solvent) and the pseudo-absorption spectrum is taken directly from the sample. Thus, the method is simple and reliable. Owing to the involvement of an extrapolation procedure, careful control of the error is needed. However, this is not critical for most spectrophotometers. Standard spectrophotometers are able to reach low enough signal-to-noise ratios to ensure reliable extrapolation. The absorption spectrum obtained results from scientific evaluation of the experimental conditions and a correct awareness of the theoretical frameworks that sustain data analysis, rather than from blind empirical procedures and intuition.

One might wonder if this method applies when using probes that absorb red light. It should be recalled that turbidity can hardly compete with a dye's absorption in this wavelength range becaue the scattering efficiency is very low and most dyes absorb light very efficiently (oscillator strengths $f \approx 1$). Nevertheless, in the particular cases where turbidity is still significant, it is possible to extend the spectrum towards the near infra-red region. Most modern standard spectrophotometers use multialkali detectors which have good performance out to 900 nm.

Materials and methods

DHE (Dehydroergosterol; $\Delta^{5,7,9(11),22}$-ergostatetraen-3β-ol; Fig. 2) was purchased from Sigma Chemical Co. (St. Louis, MO) and DPPC (dipalmitoylphosphatidylcholine) was obtained from Avanti Polar Lipids (Birmingham, AL). Both materials were used as received. Tris-HCl from BDH (London, UK) was used to prepare the buffer (Tris-HCl 50 mM, pH = 7.4, NaCl 50 mM, EDTA 0.2 mM). NaCl (p.a.) and chloroform were from Merck (Darmstadt, Germany). Deionised water was used throughout.

MLV (Multi-Lamellar Vesicles) were prepared by mixing suitable proportions of DHE and DPPC solutions in chloroform, followed by complete evaporation and hydration. SUV (Small Unilamellar Vesicles) were prepared by further sonication (carried out in three 2 min bursts using a Branson Sonifier 250 fitted with a microprobe) and separated from large vesicles and unilamellar liposomes by centrifugation (10 min at 10 000 g). For the preparation of LUV (Large Unilamellar Vesicles), MLV were extruded through two stacked polycarbonate filters (Nucleopore, 0.1 μm pore size) using an extruder (Lipex Biomembrane Inc., Vancouver, Canada). The lipid concentration in all the samples was 1.0 mM and the lipid : probe molar ratios were 10 : 1.

For the fitting of theoretical equations to experimental data we used Marquardt algorithm-based software in the "simple weighting" mode and the fitting criterion was the minimization of the χ^2 parameter (e.g. Miller and Miller 1994). This means that the optimized function is proportional to the sum of the square of the residuals, and all residuals have the same weight. This weighting mode should be used when the errors (absolute) for each data point are the same. According to our spectrophotometer manufac-

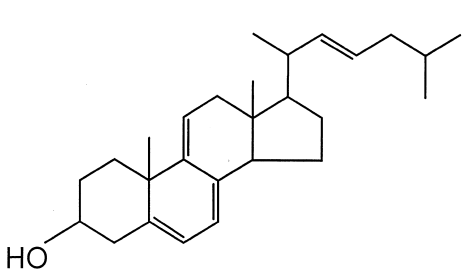

Fig. 2 Dehydroergosterol ($\Delta^{5,7,9(11),22}$-ergostatetraen-3β-ol)

[4] If B is assumed to be zero *a priori* then a linear fit can also be performed: $\ln A' = -k \cdot \ln\lambda + \ln K_0$
[5] Equations (4) and (17) should be valid over all λ values, otherwise k might be λ dependent. Slight deviations from Eq. (4) might not be totally restrictive (e.g., Kerker 1969; Wang et al. 1979)

turer (Jasco Corporation, Tokyo, Japan), the photometric repeatability (absorbancy mode) is ±0.001 up to A=0.5 and ±0.002 when 0.5<A<1. The error associated with each data point could be larger than these values (which are probably standard deviations), but still of the same order of magnitude. In any case, the errors are approximately constant over the whole A range, and thus approximately constant over the whole λ range in a spectrum, which is why simple weighting was used.

The λ interval used for data fitting was $\lambda \in$ [450 nm, 800 nm]. The results were not sensitive either to λ_{max} (limited in our system to $\lambda_{max} < 900$ nm) or λ_{min}, provided that $\lambda_{min} > 420$ nm, because dehydroergosterol absorbs below this wavelength.

Results and discussion

To check on the absence of multiple scattering (a *sine qua non* condition to apply the proposed method) we have plotted the turbidity against the lipid concentration for SUV, LUV and MLV at the lowest λ used (the worst possible scenario). The three plots are linear (data not shown) indicating the absence of significant multiple scattering.

Some results are shown in Fig. 3 (experimental spectra, fitted curves and residuals). The data refer to the sterol DHE incorporated in DPPC MLV (Fig. 3a), LUV (Fig. 3b) and SUV (Fig. 3c). The residuals are extremely small, comparable to the intrinsic error of the measurement apparatus (see Materials and Methods section). The distribution of the residuals around zero is quite satisfactory even when MLV are used. The turbidity conditions imposed by MLV are very demanding. Nevertheless, it should be stressed that the residuals are always smaller than, or approximately equal to 0.002, the intrinsic error of the apparatus. Trying to refine the statistics at this level is pointless in view of the objectives involved in this work. The residuals can be considered constant and equal to zero in all 3 cases.

MLV are large lipid vesicles with a broad size distribution (average radius ≈725 nm, Olson et al. 1979). LUV have moderately narrow size distributions with diameters approaching the pore diameter of the membrane through which they were extruded (Olson et al. 1979). In the present work, a 100 nm mean pore diameter membrane was used. SUV represent the lowest size limit possible for phospholipid vesicles. SUV of DPPC have diameters of about 25 nm (New 1990) and a narrow size distribution (Szoka 1980). DPPC refractive indexes were determined by Chong and Colbow (1976) at 20 °C and different wavelengths (n_P changes from 1.486 to 1.507 when λ changes from 366 nm to 589 nm), as well as m (m=1.115 at λ=589 nm to m=1.120 at λ=366 nm). Refractive indexes are not strongly wavelength dependent, simplifying the conclusions to be taken from the results. $\bar{m}$=1.033 was reported for egg yolk phosphatidylcholine MLV (λ=436 nm, Yoshikawa et al. 1983). The value for DPPC should be the same since the refractive index of egg yolk phosphatidylcholines at 436 nm (n_P=1.34, Yoshikawa et al. 1983) is the same as that of DPPC at the same wavelength (Chong and Colbow 1976).

The information on the refractive indexes was used along with the information available for the lipid vesicle dimensions to test whether or not the validity conditions for RG scattering are fulfilled (Eqs. (3) and (4)). λ was set to the lowest value used in this work (250 nm), representing the worst conceivable scenario in terms of the validity of Eq. (4) (i.e. the maximum possible value of $4\pi a|m-1|/\lambda$). SUV and LUV reasonably fulfil Eq. (3) and completely fulfil Eq. (4). Thus data analysis for SUV and LUV should be carried out within the framework of the RG theory. MLV do not fulfil Eq. (4) but do satisfy the conditions of Eq. (17). Therefore, data analysis for MLV should be carried out using the Mie theory (Eq. (18)).

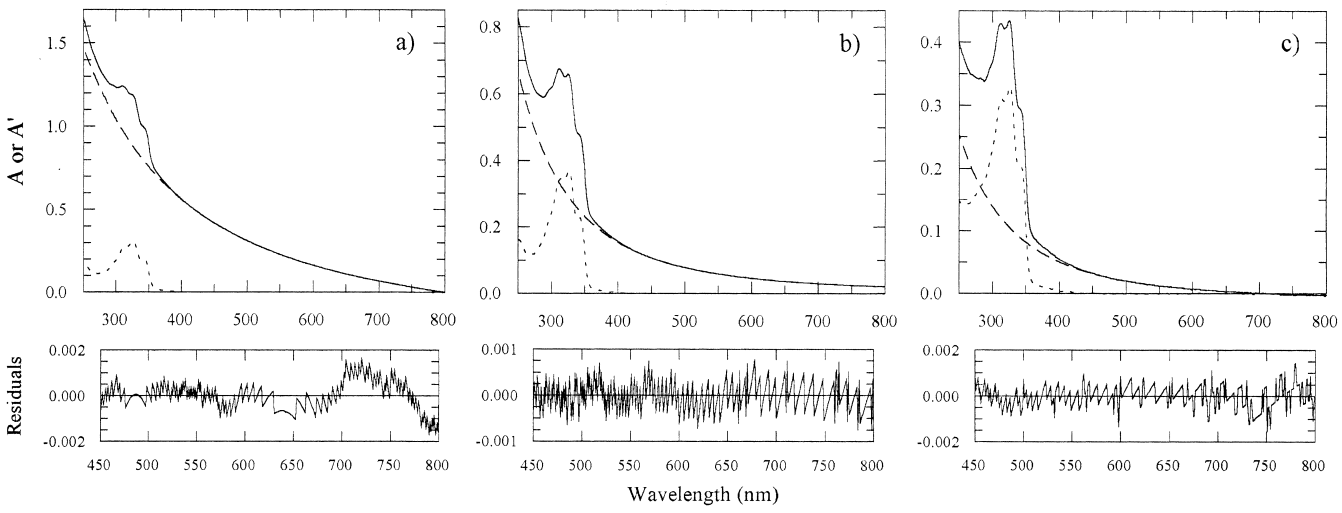

Fig. 3 Total spectrum (*solid line*), extrapolated pseudo-absorption spectrum (*long dash*) and subtraction ("true" absorption) spectrum (*short dash*) of dehydroergosterol incorporated in MLV (**a**), LUV (**b**) and SUV (**c**) of DPPC. The three subtraction spectra are superimposed in Fig. 4. Absolute residuals are plotted along λ in the *lower boxes*

Table 1 Fitting parameters values which result from the fitting of $A' = B + K_0 \lambda^{-k}$ to the λ range of the turbidity spectrum where absorption does not occur. The samples consist of MLV, LUV and SUV of DPPC (1 mM) with DHE (lipid: probe molar ratio of 10 : 1). K_0 units are nm^{-k}. B was negligible in all cases

Sample	K_0	k
MLV	1×10^4	1.56
LUV	2×10^7	3.14
SUV	8×10^6	3.12

The power parameter, k, is smallest for the MLV, having a value intermediate between 2 and 1. Thus, the data support what is expected from Eq. (18); a broad size distribution is present and a power parameter lower than 2 is due to polydispersity. With LUV and SUV values close to k=4 (although smaller than 4, probably due to some polydispersity of the size distributions) are obtained, as predicted in the RG theory. K_0 is smaller for SUV than for LUV indicating a smaller size (the w^2 effect superimposes on the N effect in Eq. (6)). B is negligible in either case.

The "true" absorption spectra obtained from SUV, LUV and MLV are shown in Fig. 4, along with a DHE absorption spectrum obtained in a homogenous solvent (chloroform) for the sake of comparison. The intensities of the four spectra are not directly comparable because in all the four cases the chromophores may experience different environments. Changes in the curvature radius in lipidic bilayers imply different physical properties such as packing density, molecular organisation and hydration. These variations may affect the oscillator strength. The deviation shown for SUV at shorter wavelengths does not seem to result from problems in extrapolation because the distribution of the residuals for the fit suggests a good quality fit.

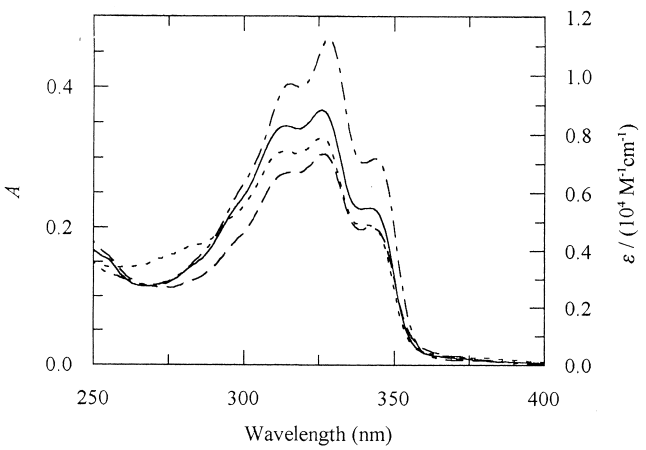

Fig. 4 Absorption spectra of DHE in MLV (*long dash*), LUV (*solid line*) and SUV (*short dash*) calculated by the procedure proposed in the text (left-hand side ordinate axis). A spectrum recorded directly in a homogenous solvent (chloroform) is also plotted for the sake of comparison (alternate short and long dashes; right-hand side ordinate axis)

Conclusions

The method outlined in this work yields reliable absorption spectra in moderately turbid media consisting of lipid vesicles or cells. It is simple, inexpensive and can be applied to data from ordinary spectrophotometers. No technical improvements are necessary. Data collection and experiment design are not altered (except to extend the λ range of spectra). Data analysis only demands a simple non-linear regression procedure which can be achieved with a wide variety of commercial software [4].

Acknowledgements The authors acknowledge Dr. M. J. E. Prieto (Technical Univ. of Lisbon, Portugal) for his valuable collaboration and JNICT (Portugal) for financial assistance (Projects Eureka – PUEM/S/ERC/93 and PECS/C/SAU/144/95). L. M. S. L. and N. C. S. acknowledge grants BD 3927/94 and BD 5935/95, respectively, from PRAXIS XXI (Portugal).

References

Barber PW, Wang DS (1978) Rayleigh-Gans-Debye applicability to scattering by nonspherical particles. Appl Opt 17:797–803
Bonner RF, Nossal R, Havlin S, Weiss GH (1987) Model for photon migration in turbid biological media. J Opt Soc Am A 4:423–432
Chong CS, Colbow K (1976) Light scattering and turbidity measurements on lipid vesicles. Biochim Biophys Acta 436:260–282
Fantini S, Franceschini MA, Fishkin JB, Barbieri B, Gratton E (1994) Quantitative determination of the absorption spectra of chromophores in strongly scattering media: a light-emitting-diode based technique. Appl Opt 33:5204–5213
Kerker M (1969) The scattering of light and other electromagnetic radiation. Academic Press, New York
Loew LM (ed) (1988) Spectroscopic membrane pbores, vol. I. CRC press, Boca Raton, Florida
Miller JC, Miller JN (1994) Statistics for analytical chemistry, 3rd edn. Ellis Horwood PTR Prentice Hall, London
New RRC (1990) Introduction. In: New RRC (ed) Liposomes – a practical approach. Oxford University Press, Oxford, pp 1–32
Olson F, Hunt CA, Szoka FC, Vail WJ, Papahadjopoulos D (1979) Preparation of liposomes of defined size distribution by extrusion through polycarbonate membranes. Biochim Biophys Acta 557:9–23
Schmitz KS (1990) Dynamic light scattering by macromolecules. Academic Press, San Diego
Szoka F, Papahadjopoulos D (1980) Comparative properties and methods of preparation of vesicles (liposomes). Ann Rev Biophys Bioeng 9:467–508
van de Hulst HC (1981) Light scattering by small particles, Dover, New York
Wang D-S, Chen HCH, Barber PW, Wyatt PJ (1979) Light scattering by polydisperse suspensions of inhomogenous nonspherical particles. Appl Opt 18:2672–2678
Wu J, Feld MS, Rava RP (1993) Analytical model for extracting intrinsic fluorescence in turbid media. Appl Opt 32:3585–3595
Yang KC, Hogg R (1979) Estimation of particle size distributions from turbidimetric measurements. Anal Chem 51:758–763
Yoshikawa W, Akutsu H, Kyogoku Y (1983) Light-scattering properties of osmotically active liposomes. Biochim Biophys Acta 75:397–406